

# Geophysical Interpretation of Possible Gold Mineralization Zones in Kyerano, South-Western Ghana Using Aeromagnetic and Radiometric Datasets

David Dotse Wemegah<sup>1,2</sup>, Kwasi Preko<sup>1</sup>, Reginald Mensah Noye<sup>1</sup>, Benjamin Boadi<sup>1</sup>, Aboagye Menyeh<sup>1</sup>, Sylvester Kojo Danuor<sup>1</sup>, Thomas Amenyoh<sup>3</sup>

<sup>1</sup>Geophysics Section, Department of Physics, Kwame Nkrumah University of Science and Technology, Kumasi, Ghana

<sup>2</sup>HydroGeophysics Group (HGG), Department of Earth Sciences, University of Aarhus, Aarhus, Denmark

<sup>3</sup>Department of Earth Sciences, University of Ghana, Legon, Ghana

Email: [ddwemegah@gmail.com](mailto:ddwemegah@gmail.com), [ddwemegah.cos@knust.edu.gh](mailto:ddwemegah.cos@knust.edu.gh)

Received 28 April 2015; accepted 27 June 2015; published 30 June 2015

Copyright © 2015 by authors and Scientific Research Publishing Inc.

This work is licensed under the Creative Commons Attribution International License (CC BY).

<http://creativecommons.org/licenses/by/4.0/>



Open Access

---

## Abstract

Airborne magnetic and radiometric datasets are used to interpret the geology and geological structural patterns which serve as potential gold mineralization zones in the Kyerano area located at south-western boundary of the prospective Sefwi Gold Belt and the Kumasi Basin in south-western Ghana. The geophysical data processing approach adopted concentrated on mapping geological boundaries, geological structures and possible gold mineralization zones is link to hydrothermally altered zones. The application of the enhancement filtering algorithms such as the reduction to the pole and analytic signal to the magnetic data, as well as the ternary radiometric image aided in the mapping of the mafic metavolcanics, basin metasediments and the belt-type granitoid complexes. The first vertical derivative and tilt angle derivative filters helped to delineate fractures, folds, and the contact zones of the formations such as that of the metavolcanics-metasediments that host the main Bibiani Shear Zone. Lineament analysis of the structures using rose diagram, reveals two main tectonic episodes in the area. These are NE-SW and NNW-SSE trending regional structures which account for about 90% of the extracted structures and are associated with the D1 and D2 deformational episodes of the Birimian Formation respectively. These structures are major fracture systems and play a pivotal role in the localization of gold mineralization in the study area.

## Keywords

Aeromagnetic, Aeroradiometric, Fault, Shear Zones, Structures

## 1. Introduction

The mining industry contributes largely to the economy of Ghana, with the country benefitting substantially from “the 10-year gold bull market” [1]. It was estimated that the sector contributed 5.7% to 6.3% to the gross domestic product (GDP) of Ghana in the period 2007 to 2011 [2] [3] and served as major foreign exchange earner for the country. The increase in the price of the commodity has also led to upsurge in illegal small-scale artisanal mining activities known locally as “galamseye”. These activities have spread throughout the gold mining areas and employed an estimated 50,000 - 200,000 number of people [4]. Small-scale miners are primarily self-employed indigenous youth, with little financial backing and limited mining expertise and are in the practice of discreetly gathering minerals found either at or just below the soil surface and selling them in contravention of state laws [5]. The activities of these people lead to the contamination of the top soil and have the further consequential effect of rendering the application of the traditional exploration methods mainly, stream and soil geochemistry ineffective.

In order not to lose the benefit the national economic derive from this sector, due to this activity there is the need to find an alternative method which is more efficient and environment friendly. This paper hence uses geophysical methods mainly airborne magnetic and radiometric for gold prospecting.

Airborne magnetic and radiometric surveys have been used extensively in the mineral exploration industry predominantly for the delineation of mineralization zones and metalliferous deposits in most parts of the world and as secondary tool in gold exploration Ghana [6]-[8]<sup>1</sup>. The successes of these methods are derived from the unique signatures that are produced by the mineralization zones making it possible to distinguish them from the host rocks. Lo and Pitcher [9] reported that mineralization in the south-western part of Ghana was hosted mostly in and at the contact zones of the metavolcanics, metasediments and Tarkwaian conglomerate associated with sericite alteration, with a potassium enrichment signature. They make it feasible to apply magnetic and radiometric methods since mafic and ultramafic igneous and metamorphic rocks typically contain the greatest abundance of magnetic minerals (high magnetic susceptibilities), radiometric minerals sedimentary rocks and sediments which typically contain the least abundance of most of these minerals [10]. Anomalies related to faults are produced by a significant contrast in magnetic properties of rocks or sediments that are juxtaposed at a fault. They make the application of geophysical methods (magnetic and radiometric) very successful in the exploration for gold in Ghana due to the distinct signatures they produce in these datasets.

In particular, the aeromagnetic method as the geophysical technique is deployed because the metavolcanics and metasediments of the Birimian Formation (the Kyerano area) contains magnetite [11], which is a common accessory mineral found in many other apatite deposits around the world [12]. Magnetic properties of rocks and sediments are determined by the quantity of magnetic minerals (iron, nickel and cobalt bearing minerals), the mode and age of the formation, and their thermal and geochemical history [13]. Similarly airborne radiometric survey is used to measure variations in the mineral composition [14], properties of soils and their parent geological material in order to map lateral lithological changes. This method involves the measurement of naturally occurring uranium (U), thorium (Th) and potassium (K), which could be found as trace elements that exist in rock forming minerals and soil profiles. In the magnetic and radiometric survey, the quantity of magnetic minerals appears to be the primary variable determining magnetic-field variations (measured as magnetic susceptibility) whereas the gamma ray responds from the radioelements (K, U and Th) in the rocks can be related to the distribution of regolith materials in Kyerano respectively.

## 2. Materials and Methodology

### 2.1. Location and Physiography of Study Area

The Kyerano area is about 90 km, southwest of Kumasi the capital of the Ashanti Region and its northern boundary is about 4 km south of the Bibiani mining operations. The study site with an area cover of about 2500 km<sup>2</sup> (Figure 1) is in the Western Region of Ghana, very close to the boundary of the Ashanti Region. The area is defined by (2.8193°W, 6.3044°N) and (2.3733°W, 6.3044°N) coordinates with projection coordinates referenced to the World Geographic System (WGS) 84 and Longitude-Latitude categories.

The area is along the prominent, NNE trending Bibiani Range, a very hilly terrain with peak heights just above 600 m above sea level and with average relief of about 300 m. The area experiences abundant rainfall

<sup>1</sup>Aerogeophysical Data for Mapping Potential Gold Mineralization Zones.

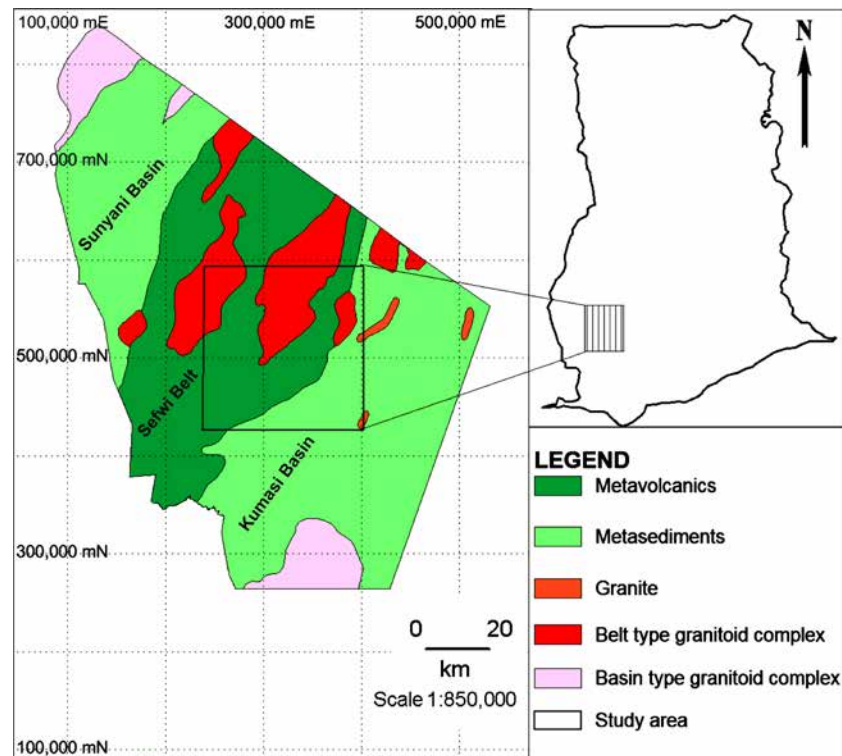


**Figure 1.** Kyerano study area showing location and geology (Modified from [11]).

(close to 2000 mm/yr) and a considerable portion of the study area falls within the TanoSuraw Forest Reserve, which displays some luxuriant primary tropical forest featuring a variety of large, high canopy trees common to the deciduous tropical forests of southern Ghana.

## 2.2. Geology, Metamorphism and Mineralization

Almost 45% of Ghana's territory belongs to the shield area consisting of Lower Proterozoic volcanic and flyschoid meta-sediments of the Birimian Supergroup [11]. The volcanics and sediments were deformed, metamorphosed and intruded by syn- and post-granitoids during the Eburnean Orogeny [11] which has led to current formation of metavolcanics, metasediments, and basin and belt type granitoid complexes (Figure 1). Kyerano lies along the central western margin of the Sefwi volcanic belt and it covers about 70 km of strike-length along the very prospective, fault bounded contact between the volcanic belt [14] and the adjacent Kumasi Basin in south-western Ghana. The western part of the area is dominated by thick sequences of mafic metavolcanics rocks that form much of the Bibiani Range [15] whereas the lower lying areas to the east are dominated by argillaceous and volcanoclastic facies of the Kumasi Basin metasediments. The central part of the area host massive belt-type granitoids which form non-foliated discordant to semi-discordant bodies [11] within the metavolcanic sequences. There are also some granitic intrusions within the area. All units have been metamorphosed to greenschist facies, which display a dominant NNE trending, steeply-dipping foliation [14].

The gold mineralization is closely associated with quartz stockwork systems hosted mainly in granitoids, occurring within the veins and in the adjacent, highly altered country rock; the high-grade zones are usually accompanied by abundant (up to about 5%) pyrite [16]. The alteration within the mineralization zones appears to consist mainly of silica, albite, sericite and iron-rich carbonate, along with fine-grained hematite and magnetite [14]. The gold occurs in very fine grains, closely associated with pyrite and appears to have been introduced along with carbonate and sulphur, which post-date the earlier alteration such as silica, sericite, iron oxides [16].

## 2.3. Airborne Magnetic and Radiometric Data Acquisition

The data used in this work was collected as part of the mineral resource support collaboration between the Geo-

logical Survey of Finland (GKT), the Geological Survey Department of Ghana and the Ghana Minerals Commission in the years 1997-98 leading to the systematic airborne geophysical survey in southern Ghana, which the Sefwi belt and Kumasi basin were part. Among the airborne geophysical datasets collected include magnetic, radiometric and electromagnetic datasets.

The airborne survey was carried out using Cessna Titan 404 (C-FYAU) fixed-wing aircraft with Scintrex Cesium SC-2 magnetometer for the magnetic survey. The survey was undertaken along flight-lines in a fixed direction that are separated by a fixed distance with reading taken at a fixed time interval, with the aircraft speed defining the sample distance along the ground.

Airborne radiometric surveys based on the measurement of gamma rays emitted with the decay of naturally occurring radioactive elements, principally from potassium (K), thorium (Th) and uranium (U) in the shallow soil/rock profile are used to map the distribution and properties of soil or landscape units particularly in the mineral exploration industry. Since gamma-rays are strongly attenuated, most of the radiation emanates from shallow ground depth, with 90% of measure gamma-rays received from the top 30 - 45 cm for a dry overburden of density 1.5 g/cm<sup>3</sup> [17]. Aeromagnetic surveys measure the total intensity of the Earth's magnetic field. The effects of Earth's primary magnetic field are removed to produce magnetic anomaly data that isolate subtle variations related to geology. These subtle variations are produced by the distribution of magnetic minerals (normally magnetite) in the ground. The distributions are commonly related to particular rock types.

All the data were gridded using minimum curvature algorithm at ¼ the flight spacing. Advance filtering algorithm having substantially ability to increases the accuracy and resolution of geophysical datasets were applied to gridded data to provide useful information on lithology and geological structures.

## 2.4. Magnetic Data Processing

Processing of potential field data entails the application of various filters to the data in order to accentuate features that will aid in the interpretation of the data. It also involves sequential processes of editing, the application of a gridding routine, and removal of the Earth's background magnetic field. A range of imaging routines were applied to the magnetic data to visually enhance the effects of selected geologic sources using mathematical enhancement techniques [18] including analytic signal amplitude, reduction to pole, first vertical derivative and tilt angle derivative.

Since the area was located at point of low latitudes, the reduction to pole transform was applied to prevent north-south signals from dominating the data thus removing the dependence of magnetic data on the angle of magnetic inclination. This filter convert data which have been recorded in the inclined earth's magnetic field to what the data would have looked like if the magnetic field had been vertical [19]. A reduction to the pole transform will provide a symmetrical anomaly over a vertically dipping, non-remanent body and is again used as an interpretation aid under certain conditions [20].

Derivatives tend to sharpen the edges of anomalies and enhance shallow features. Thus, the smaller anomalies are more readily apparent in area of strong regional disturbances. The vertical derivative map is much more responsive to local influences than to broad or regional effects and therefore tends to give sharper picture than the map of the total field intensity. The first vertical derivative was applied to the Kyerano magnetic data to delineate high frequency features more clearly where they were shadowed by large amplitude, low frequency anomalies [19]. Enhancing the magnetic data by applying the tilt derivative helped to deduce the subtle geological boundaries of the various structures enhanced by the other filtered grids.

Analytic signal filter is useful as a type of reduction to the pole [21] which was applied to magnetic data collected from the area. This filter gives a representation of the magnetic anomaly of the causative body which depends on the location of the body (horizontal coordinate and depth) and not on its magnetization direction [22].

## 2.5. Radiometric Data Processing

In order to recognize and understand radiometric signatures associated with the host rocks important to mineralization, enhancing techniques such as composite image, ratio maps as well as potassium (K), thorium (Th) and uranium (U) maps were used. Enhanced gridded images of potassium (K), thorium (Th) and uranium (U) were developed to recognize and understand radiometric signatures associated with the host rocks alteration to correlate with the pattern and trend of the geological units. Some gold deposits show increases in K and Th, which suggest that Th was mobilized in hydrothermally altered systems [23]. Decrease in Th and an increase in K is

associated with alteration environment in variety of ore deposits [24], hence, the importance of the developing the K/Th ratio map. The ratio images were also created with the motive to remove lithological differences and effects in the data caused by variations in the soil moisture, non-planar source geometry, and errors associated with altitude correction.

A composite image in red green blue (RGB) colour model was created using Geosoft software for which potassium, thorium and uranium were assigned to red, green and blue respectively. The blue tends to reduce the poorest signal-to-noise ratio of uranium channel. The resulting images to be discussed later on comprise colours generated from the relative intensities of the three components and represents subtle variations in the ratios of the three bands. A histogram equalization to give the best colour variation was used to enhance the contrast of the individual components of K, Th and U before combining to composite image.

### 3. Results and Discussion

The most direct applications of radiometric surveys are to measure variations in the radio-elemental mineral composition and map lateral lithological changes. Magnetic surveys are based on the observations of the ambient magnetic susceptibility and use this data to determine the distribution of magnetic minerals and hence changes in lithology. Integration of these surveys was used extensively for the delineation of geologic structures and metalliferous deposits. Elevated radiometric element patterns and low magnetic susceptible areas which might have resulted from rock alterations or possible mineral deposits are delineated as potential targets for ore deposits.

#### 3.1. Residual Magnetic Intensity Map

**Figure 2** is a digital elevation model of Kyerano with the highlands located at the western (H1), north-eastern (H2) and southern part (H3) separated by low elevated regions. A moderately elevated region (L2) lies between H1 and H2 whereas a very low elevated region (L1) is observed at the south-eastern part of the area likely to accumulate weathered debris from H2 and H3. **Figure 3** is a residual magnetic intensity (RMI) map which emphasizes the intensity and the wavelengths of local anomalies. The rock formations at this low magnetic latitude

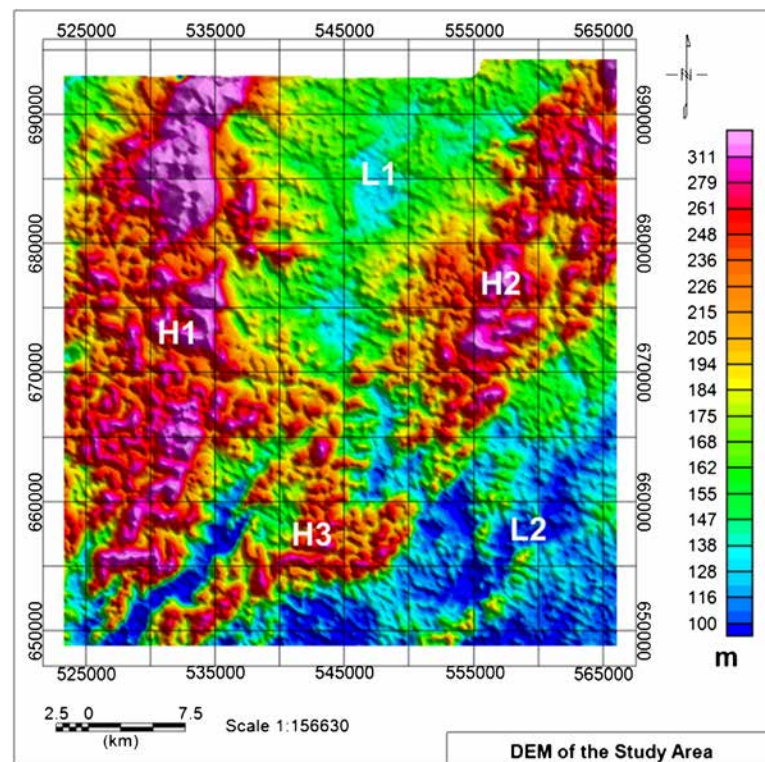


**Figure 2.** Digital elevation map of study area.

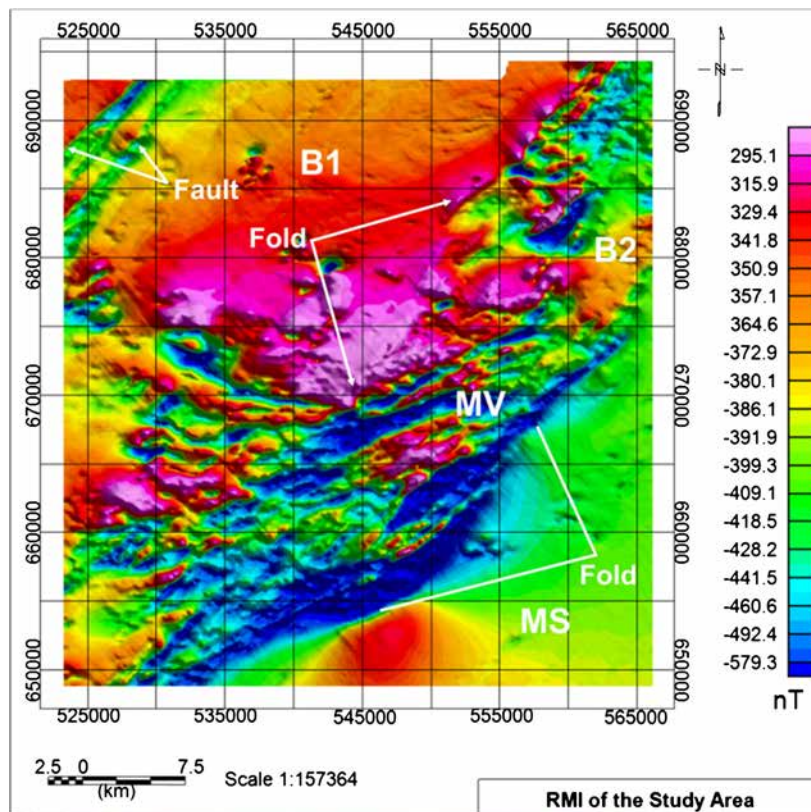


**Figure 3.** Residual magnetic intensity map.

are magnetized parallel to the Earth's magnetic field, thus most of the magnetic anomalies correlate weakly with the expected magnetic signatures of the metasediments and metavolcanics in the area.

Therefore expected high and low magnetic anomalies of the mafic and felsic rocks are represented by low and high anomalies respectively. The high elevations regions, H2 and H3 tend to lie in very low magnetic regions corresponding to the mafic metavolcanic, MV (**Figure 3**) whereas area of moderate elevation, L2 is associated with high magnetic anomaly corresponding to the belt-type granitoid B1 (expected to produce a low magnetic signature due to mainly low magnetite mineral content). The metasediments, MS (**Figure 3**) of the Kumasi basin at the lower elevation in the south-eastern corner of the area, L2 (**Figure 2**) registered low to moderate magnetic anomaly due to the low concentration of iron forming minerals and set to show similar anomaly when the data is reduced to the pole.

There is also a high magnetic signature B2 that intrudes the metavolcanic MV at the north-eastern end of the area (**Figure 3**). A change in the magnetic amplitude of B2 to low when reduced to the pole (as expected for B1) would indicate B2 as a felsic belt-type granitoid that intrudes the area. The contact zones of the belt-type granitoid (B1), metavolcanic (MV) and metasediments (MS) recorded low magnetic anomaly; an indication of demagnetization of magnetite minerals to hematite minerals with low magnetic response as a result of hydrothermal fluid flow through the fractures and faults. This is as a result of severe shearing and faulting at the boundaries of these formations. This prospective fault-bounded contact between the metavolcanics and the adjacent Kumasi Basin metasediments hosts the mineralization zone of the Kyerano Gold Mine [14].

### 3.2. Reduction-to-Pole and Analytical Signal of RMI

The features shown in the reduction to the pole transform map (**Figure 4**) resembles to a large extent the total field data except in the mafic metavolcanic (MV) where it appears to be better defined across the central part of the area. The definitive boundary and the contact zone of MV with the belt-type granitoids (B1 and B2) and basin metasediments (MS) are also well defined and appreciated as compared to **Figure 3**. The folding at the lower and upper boundary of the MS-MV contact is better defined which indicate the influence of magnetic data on

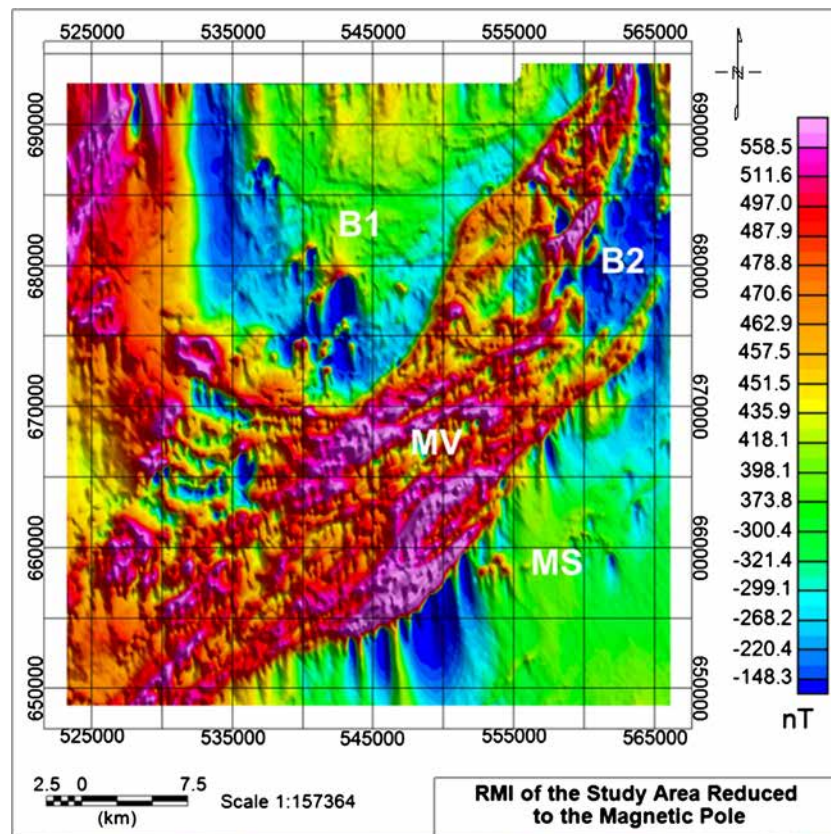


Figure 4. RMI reduced to the magnet pole.

the angle of magnetic inclination has been removed. Thus, in removing the effect of asymmetry caused by the magnetic inclination, the anomalies are better located relative to the causative bodies. After applying the RTP filter to the TMI, the host formations in **Figure 4** reflect the expected magnetic anomalies which translate into the amount of magnetic minerals (magnetite) present in the rocks, with mafic rocks showing high magnetic signature and felsic rocks (MS, B1 and B2) showing lower signatures.

The Analytic signal filter which is a form of reduction to the pole [25] was applied to the airborne residual magnetic intensity field data (RMI) to produce **Figure 5** showing the NE-SW trending MV magnetic anomaly and several distinct magnetic zones. Comparing this map (**Figure 5**), with the RMI (**Figure 4**) and the RTP colour contour maps (**Figure 3** and **Figure 4**), the difference is obvious along the edges of the metavolcanics-metasediments contact in the south-west and the central portion of the study area. The analytical signal amplitude maximizes over the edge of the magnetic structures and was used to delineate the edges of lithological units (**Figure 8**).

The high magnetic anomalies of the metavolcanics, MV and the low magnetic anomalies of B1, B2 and MS observed in **Figure 5** is indicative of the fact that the analytical signal filter is useful as a type of reduction to pole [21] when applied to magnetic data collected from low magnetic latitudes. The low magnetic anomalies of the granitic intrusive formations B3 and B4 which are similar to that of B1 and B2 were mapped better in **Figure 5** than in RTP and RMI maps. This is so irrespective of the low magnetic anomalies associated with the metavolcanic unit M1 and the belt-type granitoid B2 at the extreme north-east and north-west respectively which were both delineated by RTP and analytic signal filter.

### 3.3. Derivative Maps and Geological Structures from Magnetic Data

The computation of the first vertical derivative was to remove long wavelength features of the magnetic field and significantly improve the resolution of closely spaced and superimposed anomalies [6]. Comparison of the first vertical derivative map (**Figure 6**), with the total field map (**Figure 3**), shows a marked increase in visibility of

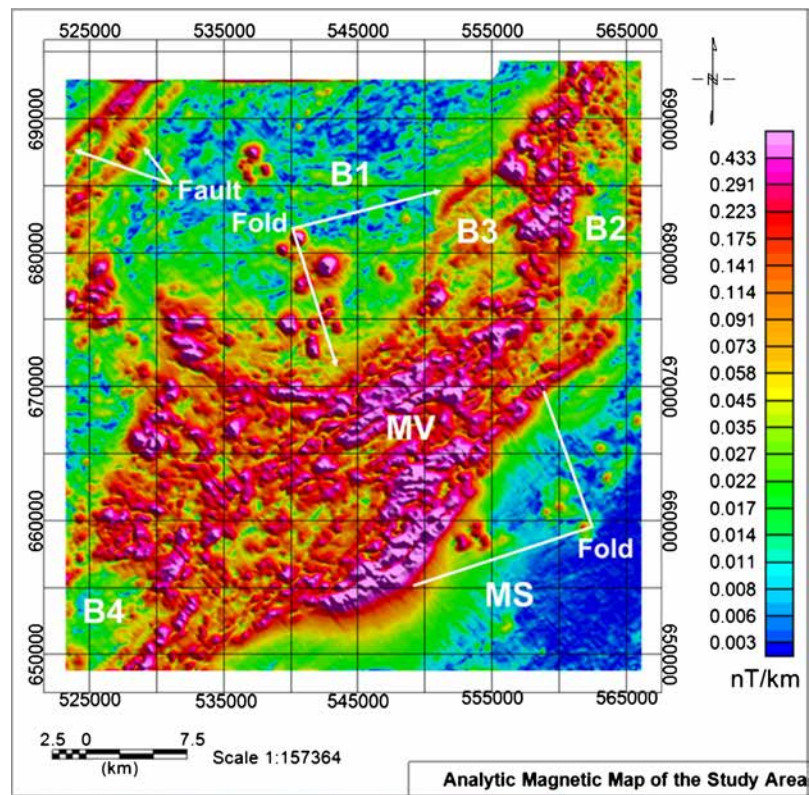


Figure 5. Analytical signal map of the RMI data.

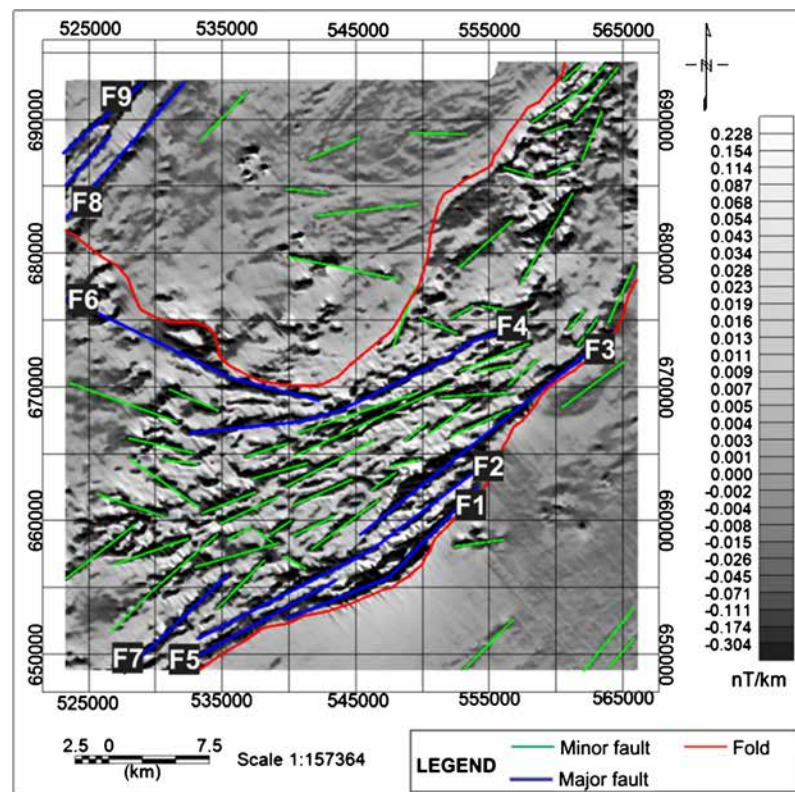


Figure 6. First vertical derivative map of magnetic data in gray scale with mapped structures.

structural features such as faults (green and blue lines), fractures and folds (red lines), especially in the southern and central part of Kyerano.

The contact zone between the metavolcanics (MV) and metasediments (MS) which hosts the main Bibiani Shear Zone and a very prominent splay fault [15] displays extensive faulting such as F1 - F1, F2 - F2, F3 - F3, F4 - F4 (Figure 6 and Figure 8) and shearing. This zone is clearly a major fracture system of regional extent [15] and it is likely to have played a fundamental role in gold mineralization. This contact zone is probably an old reactivated structure, as it appears to have guided numerous granitoid intrusions such as B2 and B4 (Figure 5 and Figure 8), which are localized along the contact zone.

The quartz stockwork systems hosted mainly in granitoids such as B1 of the TDR map (Figure 7) are closely associated with the gold mineralization [17]. The open fracture system in the granitoids most probably acted as the principal conduit for hydrothermal activity of the area in the upper part of the fault belt. The area also features a number of crosscutting faults oriented in approximately NNW to N, NE and E-W directions representing the various tectonic episodes associated with the Birimian Formation. The intruding belt-type granitoids (B1 and B3) have caused severe folding along the northern and southern boundaries of the MV and MS. The intensity of the intrusion is responsible for majority of the faults and shearing occurring along the MV-MS boundary.

The delineated geological and structural map from the magnetic data is shown in Figure 8. A large number of faults and some folds have been identified using the various filtered airborne magnetic contour maps notably the 1VD and TDR (Figure 6 and Figure 7). The intrusive granitoids have caused several and severe faults within the metavolcanics. The presence of homogenous granitoid bodies (B1, B2, and B3) have resulted in a deviation in the shear movement along the contact zone [15], and this deviation has created a zone of dilation, which became the focus of hydrothermal activity. The movement of hydrothermal fluids to low pressured zones within the fault zones generated heat which destroyed the magnetic mineral within the host rocks, thus the magnetic anomalies associated with these faults are low.

### 3.4. Radiometric Data

A number of potassium (K), uranium (U) and thorium (Th) radiometric signatures are evident in the radiometric

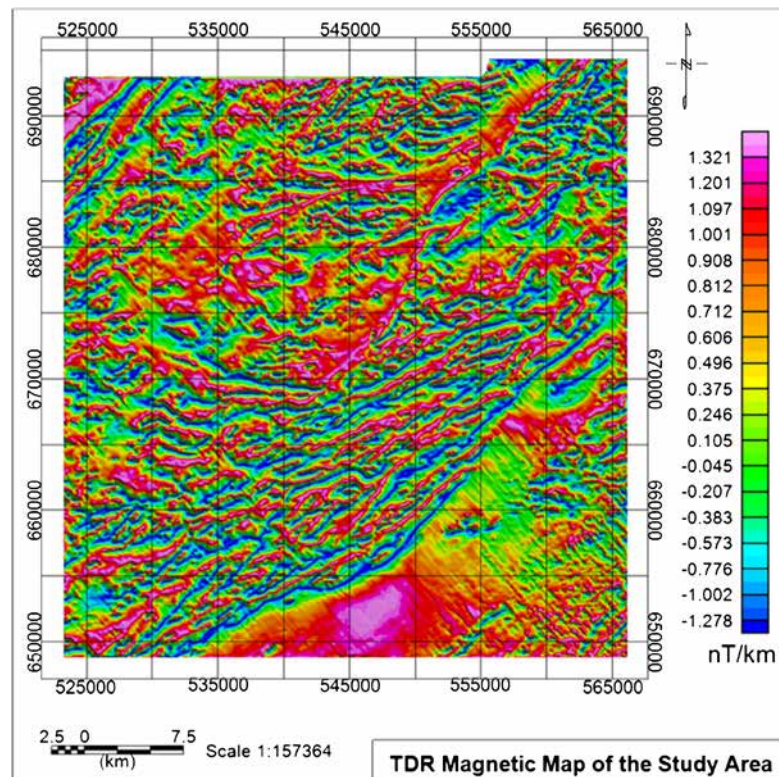
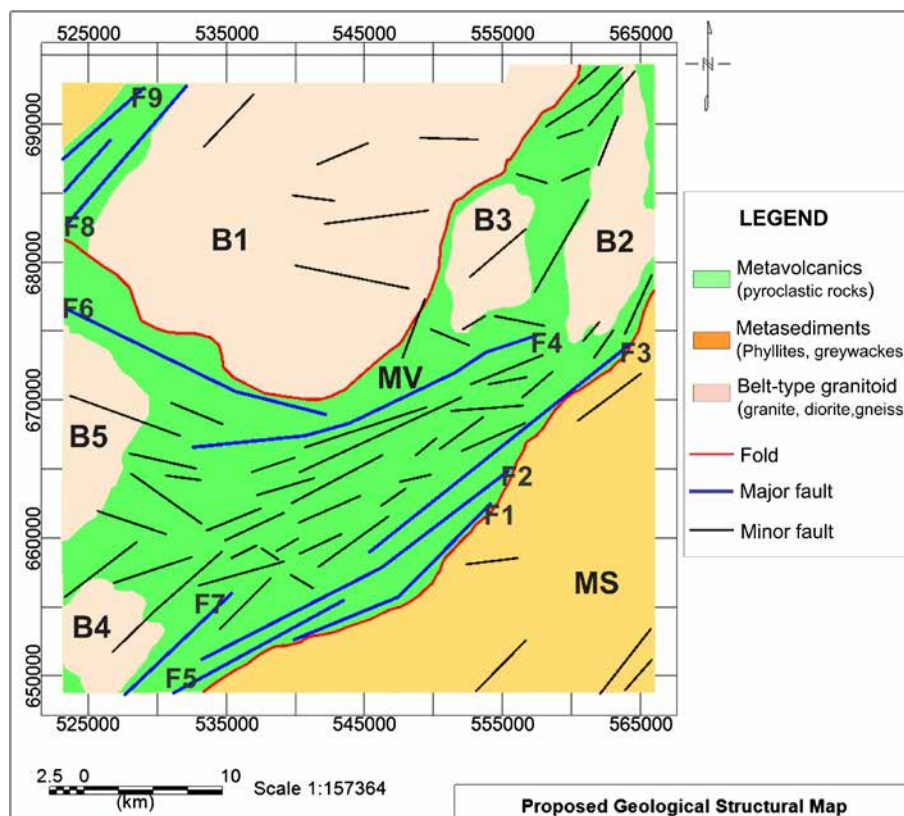


Figure 7. Tilt angle derivative of magnetic the data.



**Figure 8.** Proposed structural and geological map delineated from aeromagnetic data.

survey data. A strong K signature occurs south of the metavolcanics which is associated with the basin metasediments at the south-western part of the area (Figure 9). Potassium radiations essentially come from K feldspar, predominantly micas such as muscovite and biotite [7] which is common in the felsic regolith of the metasediments (MS) and are low in mafic rocks [26], hence the weak K signature in the metavolcanics. The metasediments also recorded weak anomalies of immobile and mobile Th and U (Figure 10, Figure 11) [23] respectively, although some high trace of these radioelements can be traced within the formation.

The western and north-eastern parts of area are associated with strong Th signature (Figure 10) and U signature (Figure 11) with the south-eastern and northern part recording weak Th and U concentrations. The metavolcanics MV show stronger Th signature (Figure 10) which distinctively defines the boundaries with the MS and the belt-type granitoids (B1, B2 and B4). Unlike the K and the Th maps, the U map could not clearly distinguish the boundary between the metasediments and metavolcanics. Comparatively, weak K and Th anomalies are recorded in the regions which correspond to the belt-type granitoids *i.e.* B1, B2, B3 and B4. Thorium is generally considered very immobile [23], thus, the regions with low thorium concentration, such as the belt granitoids and north-east contact zone of MV-MS (Figure 10) cannot be attributed to depletion due to hydrothermally altered system associated with the area.

The ratio map of K and Th (Figure 12) indicates a strong concentration of K (red colour) and this suggests low concentration of Th. Decrease in Th and an increase in K occurrence as noted along the faulted north-east metasediments-metavolcanics contact zone (Figure 6, Figure 9, Figure 10, and Figure 12) are favourable alteration environment for variety of ore deposits [24]. The ratio map (Figure 12) depicts this region marked X1 with high K (red colour) and low Th. However, some possible gold mineralization zones show increases in K and Th such as the north-east metavolcanics intrusive granitoids contact zone (X2 in Figure 12). This suggests that Th was mobilized in hydrothermally altered systems.

The highly fractured south-western fault belt which mainly occurs in the volcanic belt produced relatively low potassium signature. The contact of this region is defined by the prospective fault bounded contact between the volcanic belt and the adjacent Kumasi basin metasediments (hosting the Bibiani Shear Zone and a very prominent

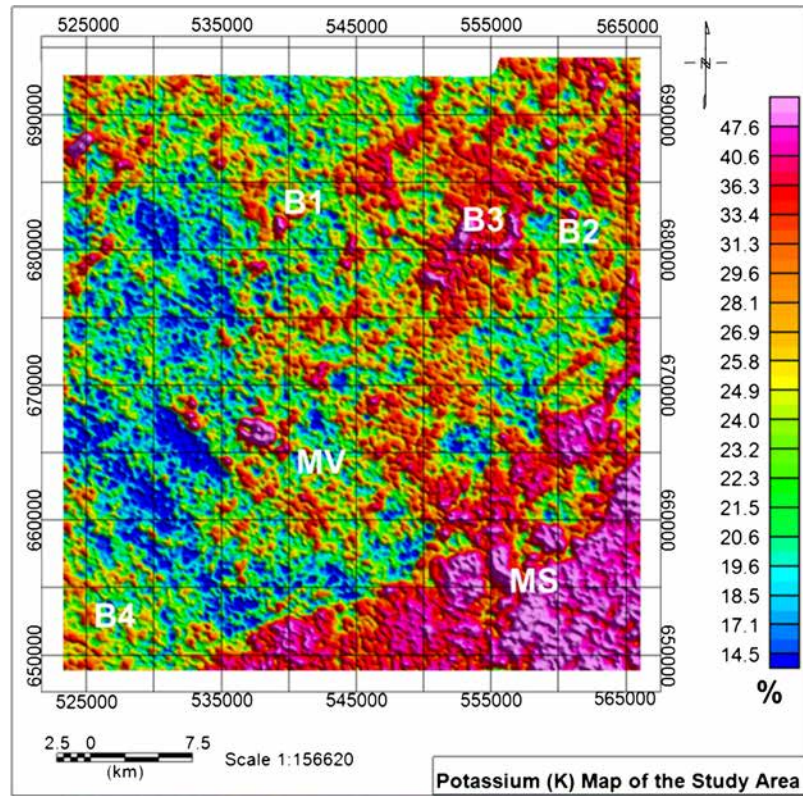


Figure 9. Potassium concentration map.

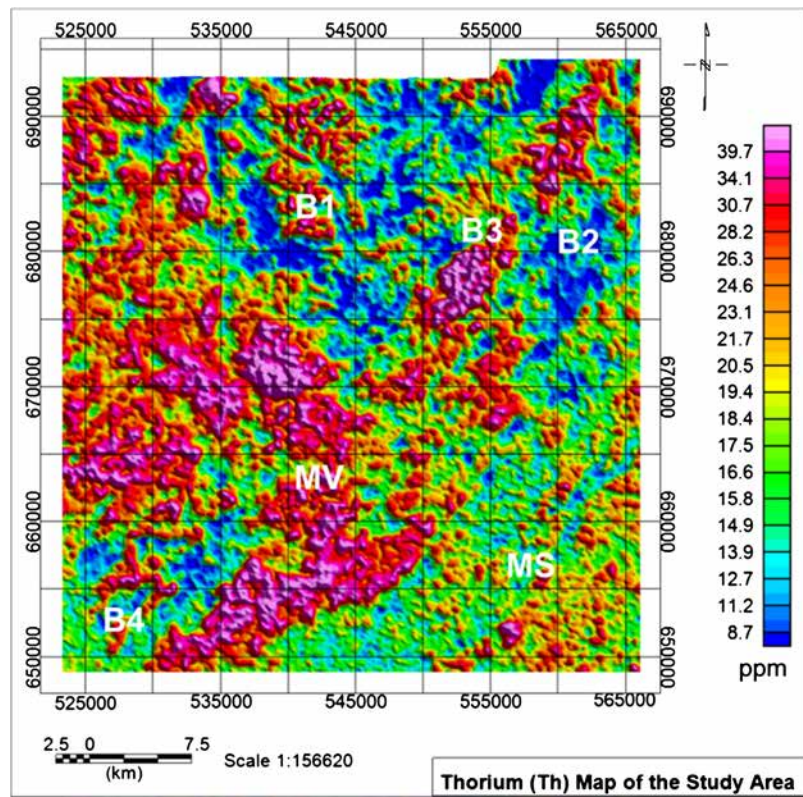


Figure 10. Thorium concentration map.

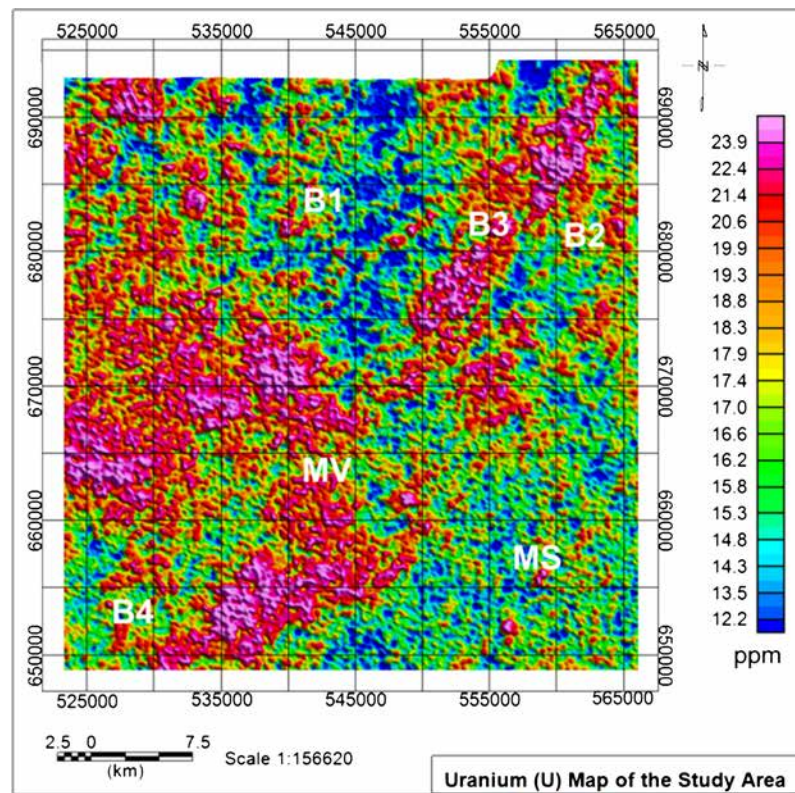


Figure 11. Uranium concentration map.

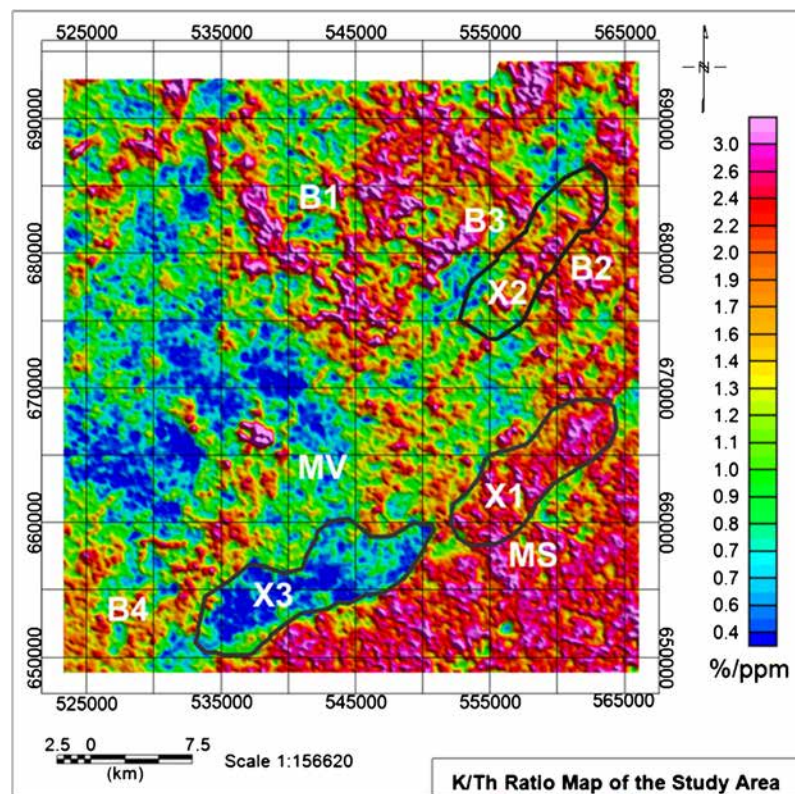


Figure 12. Potassium thorium ratio map.

splay fault (Kyerano shear) and the western metavolcanic-belt granitoid contact zone. The south-western metavolcanics-metasediments contact zone recorded weak K (**Figure 9**), strong Th and U (**Figure 10** and **Figure 11**).

The ternary image (**Figure 13**) comprises of colours generated from the relative intensities of the three components and represents subtle variations in the ratios of the three bands with K assigned to red, U to blue and Th to green. The composite image presents strong spatial correlations with the known geologic units and the most prominent features in the K, Th, and U images. The most notable units in the ternary image are the mafic and magnetite rich MV formations which are represented in cyan (**Figure 13**) and also notable in both U and Th maps (**Figure 10** and **Figure 11**). In addition, the metasediments with high K concentration and some traces of U are given a magenta colour. This strong correlation is based on the fact that the metasediments are made up of the potash-rich (high K concentration) regolith which come in the form of muscovite, biotite, aplite and pegmatite [14].

The blue-dark blue regions (**Figure 13**) are associated with the belt-type granitoids (B2, B3, B4 and the western part of B1). The K, Th and U maps show that the granitoids recorded weak anomaly of K and Th (**Figure 9** and **Figure 10** respectively) but strong U anomaly (**Figure 11**). The strong U anomaly associated with belt granitoids B2, B3 and B4 suggests that these granitoids may be younger than B1 although these granitoids had similar low magnetic anomaly or the latter may have been affected by higher alteration grade. A long denudation period of weathering has probably depleted most of the U concentration of B1 within the central and eastern part with only small trace in the western part remaining. These dark/black regions which occur within faulted zones and in some areas at the contact zones of the rock formation can be attributed to the low concentration of the K, Th and U. The white zones in the ternary image are indications of high concentration of K, Th and U whilst the yellow indicate zones of high K and Th but low U concentrations.

In order to help delineate a geological map based on the radiometric data in the present study, the radioelement ternary image (**Figure 13**) was used to first outline the major lithological units which describe different radioactivity levels. The interpreted individual units were subjected to further refinement using the potassium, Th and U composite colour images (**Figures 9-11**). **Figure 14** shows the interpreted lithologic units as inferred from the radioelement composite image.

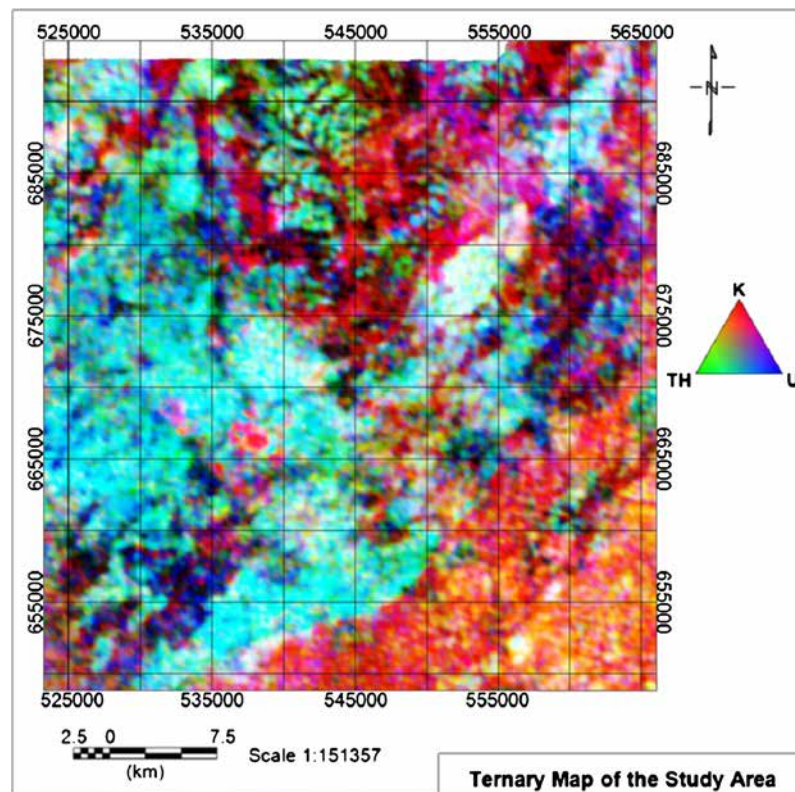


**Figure 13.** Radiometric ternary map.

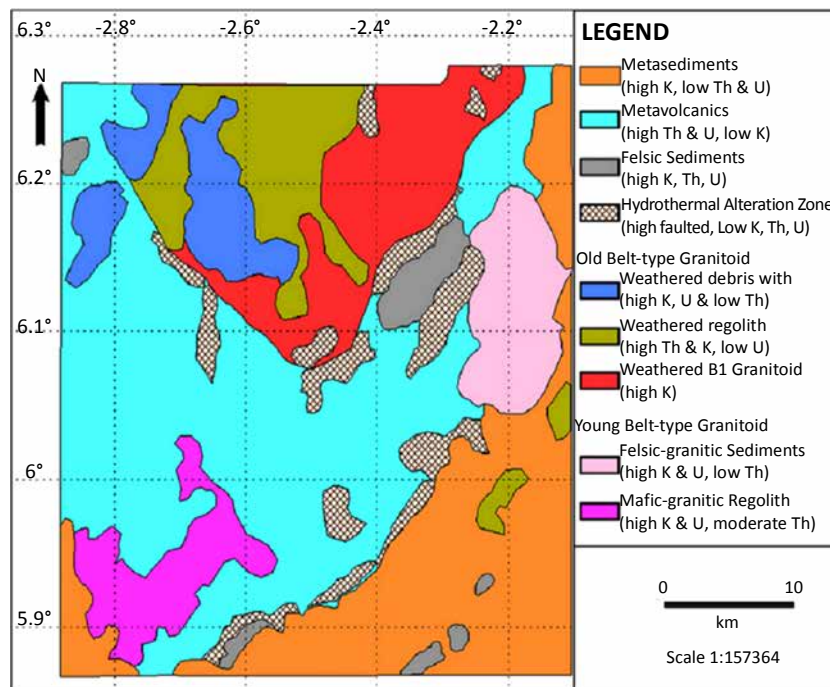


Figure 14. Lithological map interpreted from radiometric data.

### 3.5. Integrated Geological and Structural Map

The deduced geological and structural maps from the magnetic and radiometric data were integrated to produce a composite geological map of the area (Figure 15(a)). Areas of intense hydrothermal alteration which are possible zones of gold mineralization were also mapped. Delineated lineaments from the magnetic data are also shown on the map.

Lineament analysis of the mapped geological structures was carried to determine the trend of the major lithological contacts, faults and fractures in the study area. The lineament's azimuth was plotted on rose diagram to identify the dominant structural orientations that reflect the origin (Figure 15(b)) of the tectonic regime. The analysis reveals two main tectonic events *i.e.* the NE-SW trending tectonic event (D1) and the NNW-SSE trending structural deformational event (D2) constituting 96% of all structural orientation. These are the two major tectonic episodes that are associated with the Birimian Formation which are both potential hydrothermal gold mineralization zones [14].

## 4. Conclusion

The application of the enhancement filtering algorithmssuch as the reduction-to-pole and analytical signalto the magnetic data aided in the mappingof the mafic metavolcanic,basin metasediments and the belt-type granitoids lithologic units. Similarly, the application of thedirective filters to thedata helped to delineate fractures, folds, and the contact zones of the formations such as that of the metavolcanics-metasediments that host the main Bibiani Shear Zone. The lineament analysis of the structures using rose diagram, reveals two main tectonic episodes in the area. These are the NE-SW and the NNW-SSE structures, principal structure trends in the area, which account for about 96% of the extracted structures, are associated with the D1 and D2 deformational episodes of the Birimian Formations. The composite image technique applied to the radiometric data facilitates the correlation and delineation of lithological units based on subtle differences in the radioelements concentrations. These methods are successfully used in mapping the metavolcanics-metasediments contact, delineate and subdivide the belt-type granitoid, and highlight the rock types characterized by low content of radioelements. Integration of the two datasets provides the means for the successful mapping of the various geological units, their contacts zones and some hydrothermal alternation zones which are potential hydrothermal gold mineralization zones.

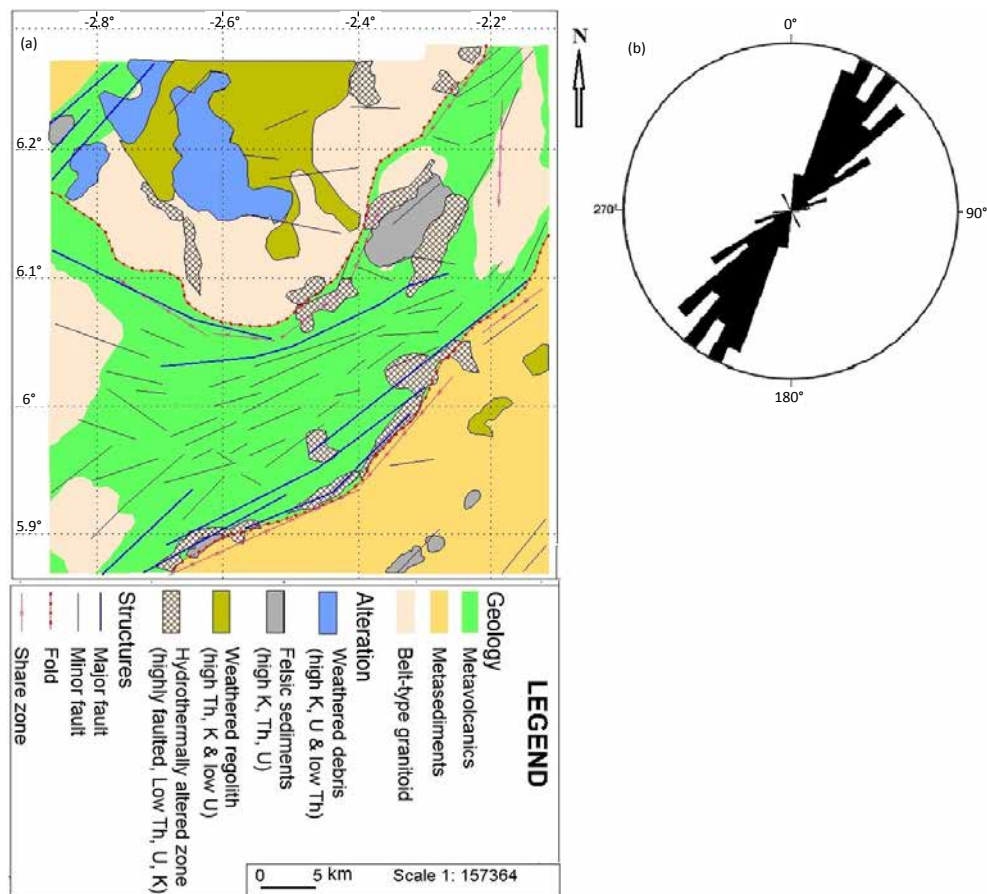


**Figure 15.** (a) Integrated geological map of the study area; (b) Rose diagram showing structural orientations in the area.

## Acknowledgements

The authors are grateful to Geology Survey Department of Ghana for making the data available for this study. We appreciate the help you have given us over the years.

## References

- [1] World Gold Council (2010) The 10-Years Gold Bull Market in Perspective.
- [2] Amankwah, R.K. and Anim-Sackey, C. (2003) Strategies for Sustainable Development of the Small-Scale Gold and Diamond Mining Industry of Ghana. *Resources Policy*, **29**, 131-138. <http://dx.doi.org/10.1016/j.resourpol.2004.07.002>
- [3] Bloch, R. and Owusu, G. (2012) Linkages in Ghana's Gold Mining Industry: Challenging the Enclave Thesis. *Resources Policy*, **37**, 434-442. <http://dx.doi.org/10.1016/j.resourpol.2012.06.004>
- [4] Hilson, G.M. (2004) Structural Adjustment in Ghana: Assessing the Impacts of Mining-sector Reform. *African Affairs*, 54-77. <http://dx.doi.org/10.1353/at.2005.0006>
- [5] Aubynn, A.K. (1997) Liberalism and Economic Adjustment in Resource Frontiers: Land-Based Resource Allocation and Local Responses. A Reflection from Western Ghana. Working Paper 9/97. Institute for Development Studies, University of Helsinki, Helsinki.
- [6] Keating, P.B. (1995) A simple Technique to Identify Magnetic Anomalies Due to Kimberlite Pipes. *Exploration and Mining Geology*, **4**, 121-125.
- [7] Boadi, B., Wemegah, D.D. and Preko, K. (2013) Geological and Structural Interpretation of the Konongo Area of the Ashanti Gold Belt of Ghana from Aeromagnetic and Radiometric Data. *International Research Journal of Geology and Mining*, **3**, 124-135.
- [8] Graham, K.M., Preko, K., Wemegah, D.D. and Boamah, D. (2013) Geological and Structural Interpretation of Part of

- the Buem Formation, Ghana, Using Aerogeophysical Data. *Journal of Environment and Earth Science*, **4**, 17-31.
- [9] Lo, B.H. and Pitcher, D.H. (1996) A Case History on the use of Regional Aeromagnetic and Radiometric Data Sets for Lode Gold Exploration in Ghana. Annual Meeting Expanded Abstracts, Society of Exploration Geophysicists, 592-595. <http://dx.doi.org/10.1190/1.1826712>
- [10] Reynolds, R.L., Rosenbaum, J.G., Hudson, M.R. and Fishman, N.S. (1990) Rock Magnetism, the Distribution of Magnetic Minerals in the Earth's Crust and Aeromagnetic Anomalies. *US Geological Survey Bulletin*, **1924**, 24-45.
- [11] Kesse, G.O. (1985) The Mineral and Rock Resources of Ghana. A.A. Balkema, Rotterdam.
- [12] Rajesh, V.J., Yokoyama, K., Santosh, M., Arai, S., Oh, C.W. and Kim, S.W. (2006) Zirconolite and Baddeleyite in an Ultramafic Suite from Southern India: Early Ordovician Carbonatite-Type Melts Associated with Extensional Collapse of the Gondwana Crust. *The Journal of Geology*, **114**, 171-188. <http://dx.doi.org/10.1086/499571>
- [13] Case, J.E., and Sikora, R.F. (1984) Geologic Interpretation of Gravity and Magnetic Data in the Salida Region, Colorado. *US Geological Survey Open-File Report*, **46**, 84-372.
- [14] Wilford, J.R., Bierwirth, P.N. and Craig, M.A. (1997) Application of Airborne Gamma-Ray Spectrometry in Soil/Regolith Mapping and Applied Geomorphology. *AGSO, Journal of Australian Geology and Geophysics*, **17**, 201-216.
- [15] Hirdes, W., Senger, R., Adjei, J., Efa, E., Loh, G. and Tetty, A. (1993) Explanatory Notes for the Geological Map of Southwest Ghana 1:100,000, Sheet Wiawso (0603d), Asafo (0603c), Kukuom (0603b), Goaso (0603a), Sunyani (0703d) and Berekum (0703c). Geologisches Jahrbuch Reihe B, Band B 83, Hannover, 139 p.
- [16] Griffis, R.J. (1998) Explanatory Notes-Geological Interpretation of Geophysical Data from South-Western Ghana. Minerals Commission, Accra, 51 p.
- [17] Grasty, R.L. (1976) Applications of Gamma Radiation in Remote Sensing. In: Schanda, E., Ed., *Remote Sensing for Environmental Sciences*, Springer Verlag, Berlin, 257. [http://dx.doi.org/10.1007/978-3-642-66236-2\\_7](http://dx.doi.org/10.1007/978-3-642-66236-2_7)
- [18] Milligan, P.R. and Gunn P.J. (1997) Enhancement and Presentation of Airborne Geophysical. *AGSO, Journal of Australian Geology and Geophysics*, **17**, 64-74.
- [19] Geosoft Inc. (1996) OASIS Montaj Version 4.0 User Guide. Geosoft Incorporated, Toronto.
- [20] Geosoft Inc. (1995) OASIS Montaj Airborne Radiometric Processing System Version 1.0 User's Guide. Geosoft Incorporated, Toronto.
- [21] Ansari, A.H. and Alamdar, K. (2009) Reduction to the Pole of Magnetic Anomalies Using Analytic Signal. *World Applied Sciences Journal*, **7**, 405-409.
- [22] Debeglia, N. and Coppel, J. (1997) Automatic 3-D Interpretation of Potential Field Data Using Analytic Signal Derivatives. *Geophysics*, **62**, 87-96. <http://dx.doi.org/10.1190/1.1444149>
- [23] Silva, A.M., Pires, A.C.B., Mccafferty, A., de Moraes, R.A.V. and Xia, H. (2003) Application of Airborne Geophysical Data to Mineral Exploration in the Uneven Exposed Terrains of the Rio Das Velhas Greenstone Belt. *Revista Brasileira de Geociências*, **33**, 17-28.
- [24] Ostrovskiy, E.A. (1975) Antagonism of Radioactive Elements in Well Rock Alteration Fields and Its Use in Aero-gamma Spectrometric Prospecting. *International Geological Review*, **17**, 461-468. <http://dx.doi.org/10.1080/00206817509471687>
- [25] Nabighian, M.N. (1984) Toward a Three-Dimensional Automatic Interpretation of Potential Field Data via Generalised Hilbert Transforms: Fundamental Relations. *Geophysics*, **49**, 780-789. <http://dx.doi.org/10.1190/1.1441706>
- [26] Manu, J. (1993) Gold Deposits of Birimian Greenstone Belt in Ghana: Hydrothermal Alteration and Thermodynamics. PhD Thesis, Braunschweiger Geologisch-Paläontologische Dissertationen, Vol. 17, Braunschweig.